Supporting Information

Feasible Constructions of Bi@CNT Materials with Extremely High Rate and Na^+ Storage Performance

Jianke Li [a], Xincheng Miao,*[c] Beibei Han [d], Kun Wang,*[a] Baigang An [a], Chengguo Sun [a], Guiying Xu,*[a] Dongying Ju [b], Lin Tao [a], Weimin Zhou,*[a]

[a] Key Laboratory of Energy Materials and Electrochemistry Research Liaoning Province, University of Science and Technology Liaoning, No. 189, Qianshan Middle Road, Lishan District, Anshan City, Liaoning Province, Anshan 114051, China.
[b] Advanced Science Research Laboratory, Saitama Institute of Technology, 1690 Fusaiji, Fukaya, Japan.
[c] School of Materials and Metallurgy, University of Science and Technology Liaoning, No. 189, Qianshan Middle Road, Lishan District, Anshan City, Liaoning Province, Anshan 114051, China.
[d] Key Laboratory of Advanced Fuel Cells and Electrolyzers Technology of Zhejiang Province, Ningbo Institute of Materials Technology and Engineering, Chinese Academy of Sciences, Ningbo, No. 1219 Zhongguan West Road, Zhejiang 315201, China.

E-mail: aszhou15242870697@163.com; asust_msn@163.com; ustl15542731203@163.com; xuguiying751107@163.com;

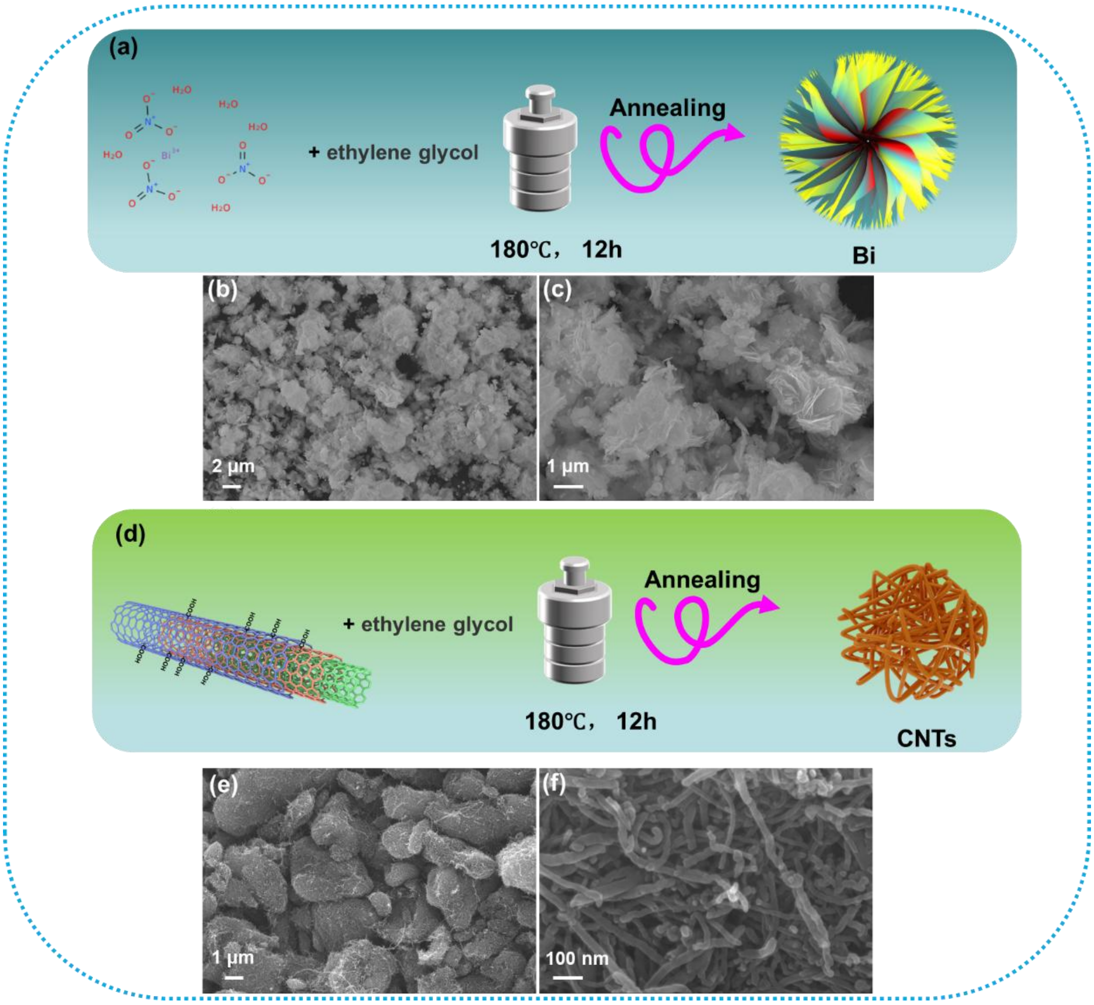

Fig. S1. (a) Synthetic schematic diagram of the pure Bi. (b, c) SEM images of pure Bi. (d) Synthetic schematic diagram of the pure CNTs. (e, f) SEM images of pure CNTs.

$$Bi\ (wt.\%)=2\times\frac{\text{final weight of } Bi_2O_3}{\text{molecular weight of } Bi_2O_3}\times\frac{\text{molecular weight of Bi}}{\text{initial weight of Bi@CNT}}\times 100\%$$

Equation S1

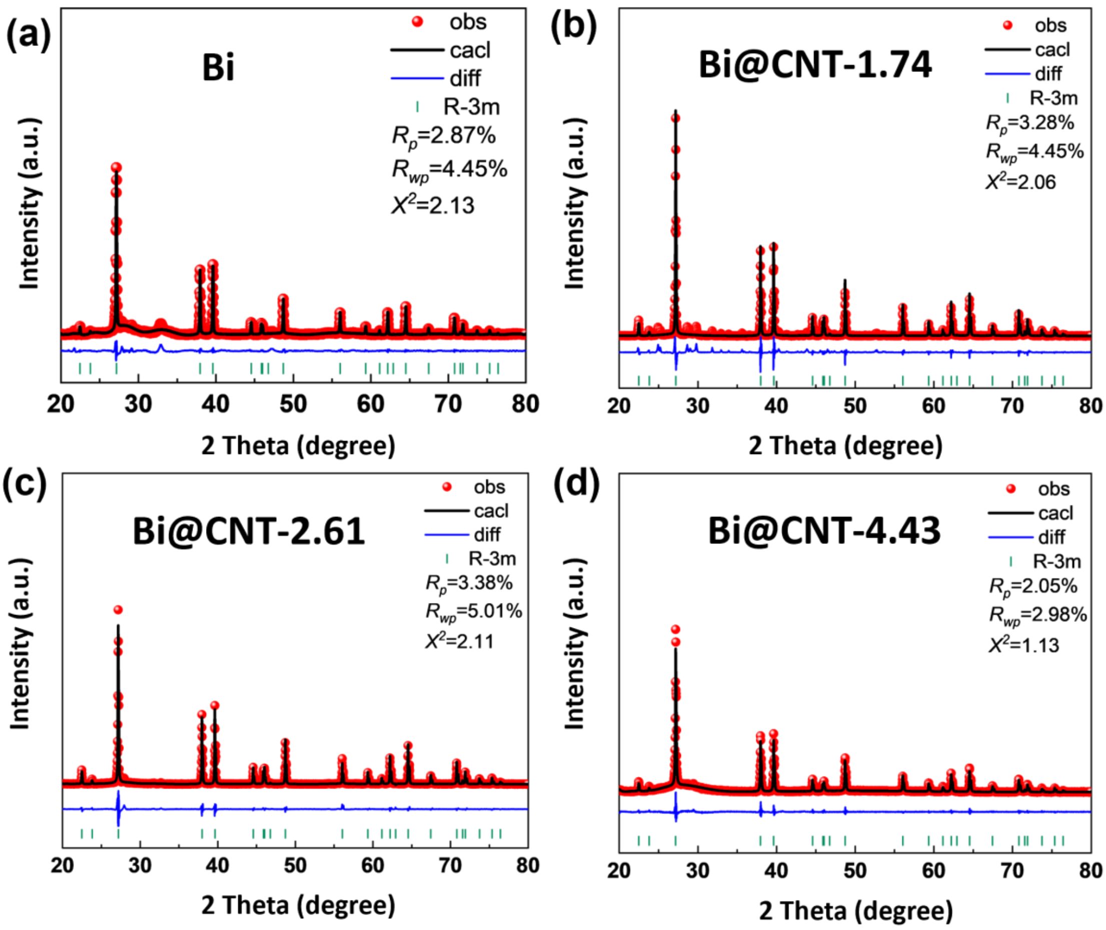

Fig. S2. XRD patterns with the Rietveld refinement of Bi (a), Bi@CNT-1.74 (b), Bi@CNT-2.61(c) andBi@CNT-4.43(d).

Table S1. Structural parameters of Bi, Bi@CNT-1.74, Bi@CNT-2.61 and Bi@CNT-4.43 materials from Rietveld refinement.

Samples	a (Å)	b (Å)	c (Å)	Vol. (Å^3)	Micro strain
Bi	4.5453	4.5453	11.8577	212.159	995.5
Bi@CNT-1.74	4.5458	4.5458	11.8616	212.276	1547.0
Bi@CNT-2.61	4.5461	4.5461	11.8619	212.308	938.4
Bi@CNT-4.43	4.5446	4.5446	11.8576	212.092	1109.3

Table S2. Carbon contents in Bi@CNT materials determined by elemental analyses.

Samples	Wt.(%)
Bi@CNT-1.74	11.08
Bi@CNT-2.61	8.82
Bi@CNT-4.43	5.27%

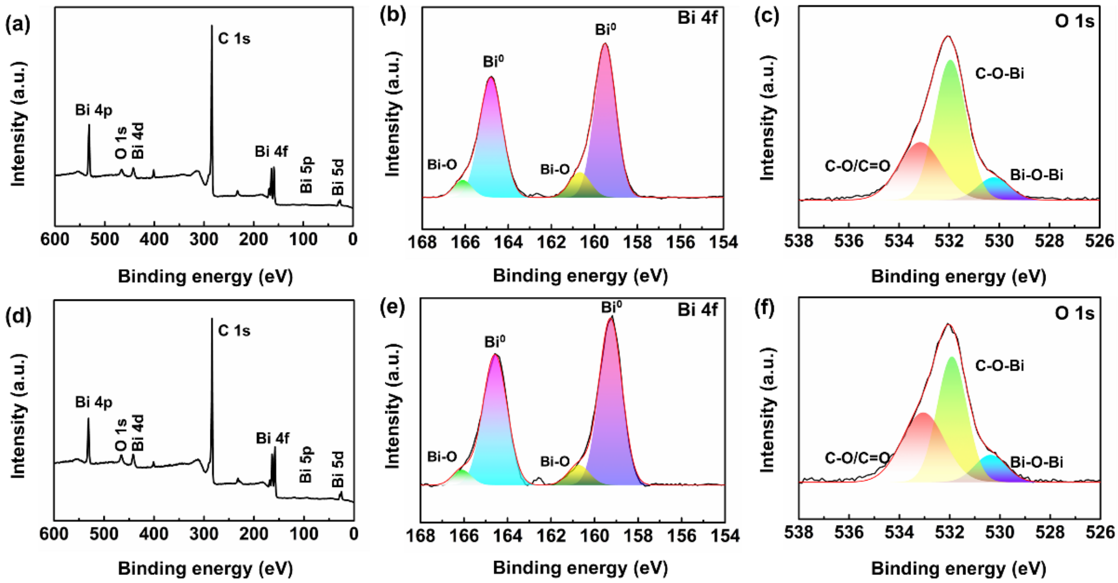

Fig. S3. XPS spectra of Bi@CNT-1.74 (a-c) and Bi@CNT-4.43 materials (d-f).

Table S3. The contents of chemical bonds in O 1s spectra of Bi@CNT materials.

Samples	Chemical bond	Content (%)
Bi@CNT-1.74	Bi-O-Bi	32.14
	C-O/C=O	9.46
	C-O-Bi	58.40
Bi@CNT-2.61	Bi-O-Bi	25.58
	C-O/C=O	6.99
	C-O-Bi	67.43
Bi@CNT-4.43	Bi-O-Bi	39.22
	C-O/C=O	49.26
	C-O-Bi	11.52

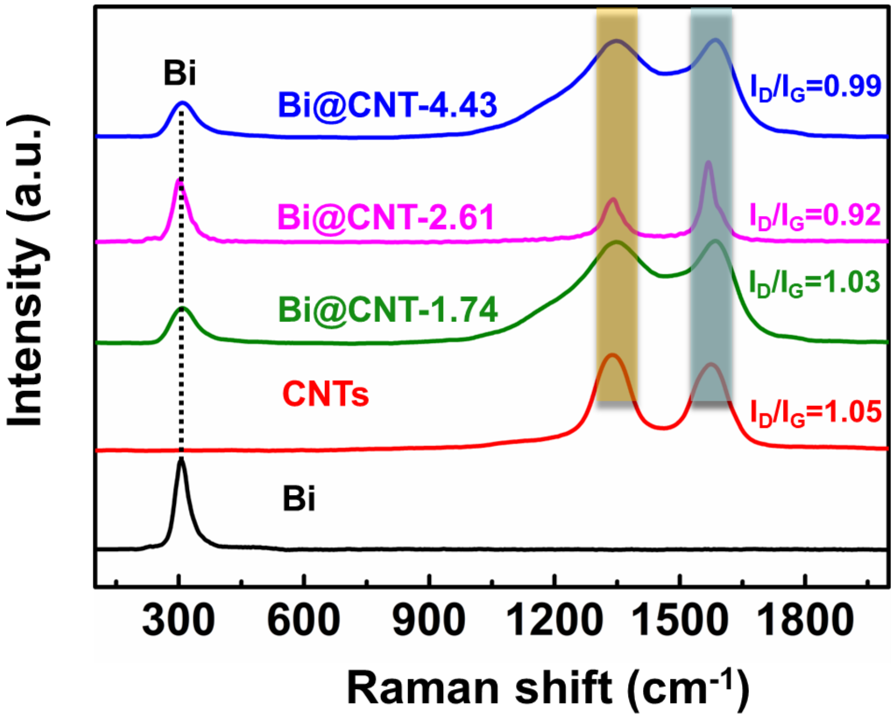

Fig. S4. Raman spectra of Bi, CNTs, and Bi@CNT materials.

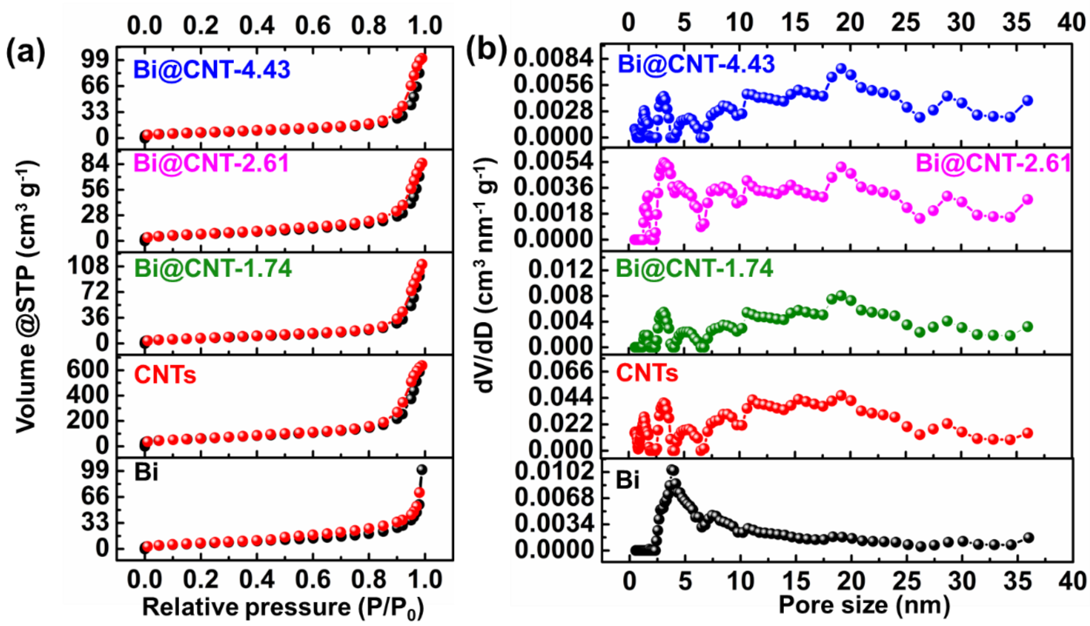

Fig. S5. (a) Nitrogen adsorption-desorption isotherms and (b) pore size distributions of Bi, CNTs, and Bi@CNT materials.

Table S4. Information on the specific surface area and total pore volume of the Bi, CNTs, and Bi@CNT.

Samples	S_{BET} (m^2/g)	Total Pore Volume ($cm^3\ g^{-1}$)
Bi	26.69	0.150
CNTs	218.98	0.098
Bi@CNT-1.74	26.38	0.017
Bi@CNT-2.61	26.42	0.013
Bi@CNT-4.43	24.73	0.016

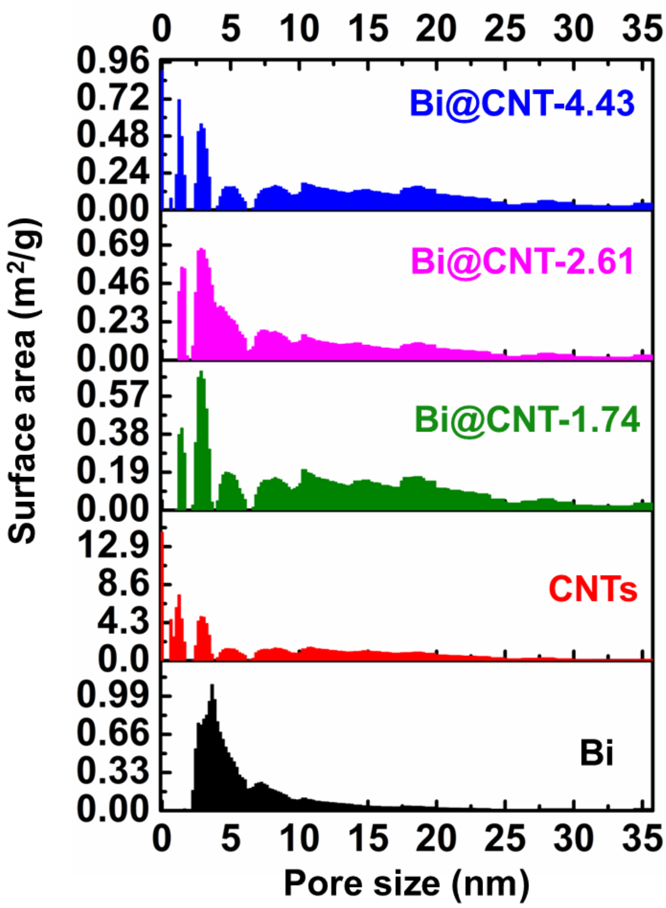

Fig. S6. The relationships between surface area and pore size of Bi, CNTs, and Bi@CNT materials.

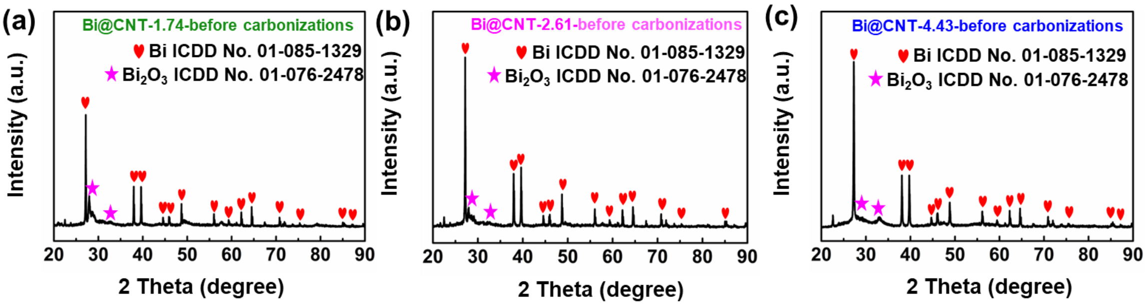

Fig. S7. (a-c) are the XRD patterns of uncarbonized Bi@CNT-1.74, Bi@CNT-2.61, and Bi@CNT-4.43, respectively.

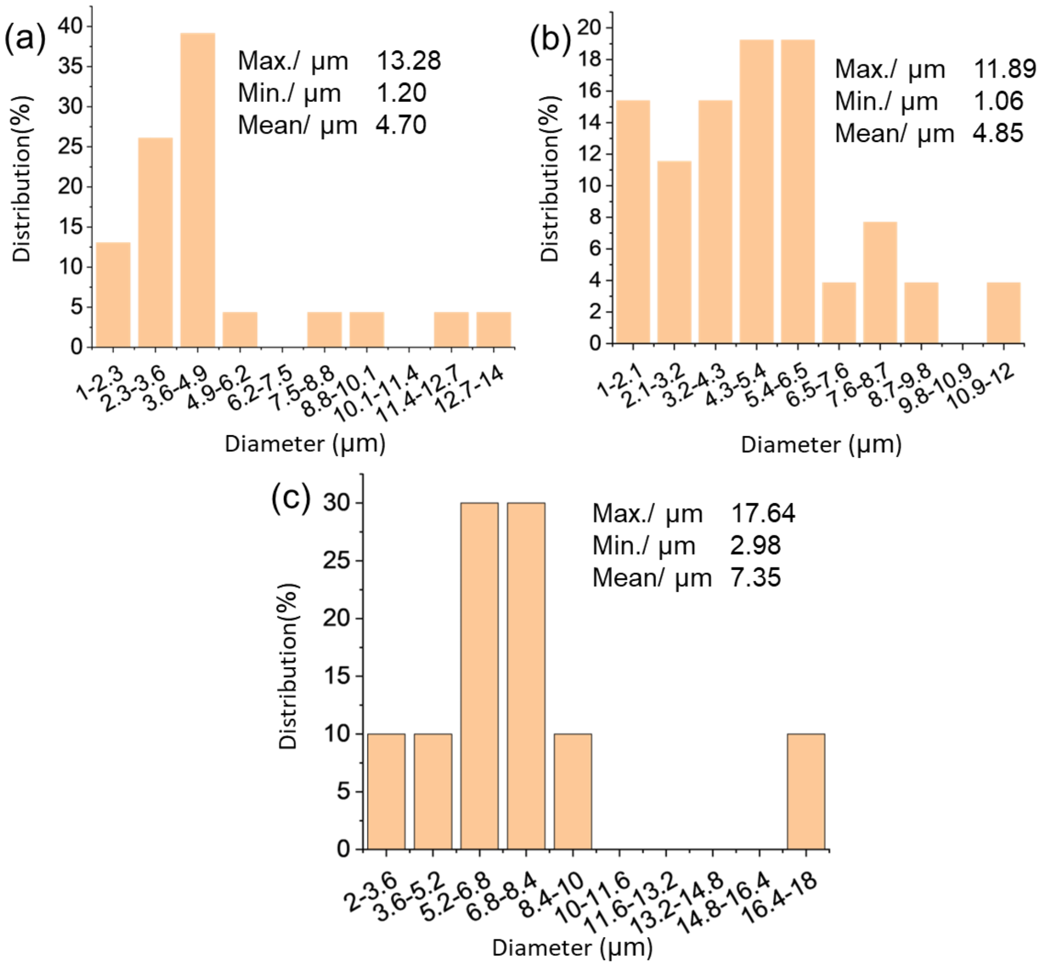

Fig. S8. (a-c) are the particle size distributions of carbonized Bi@CNT-1.74, Bi@CNT-2.61, and Bi@CNT-4.43, respectively.

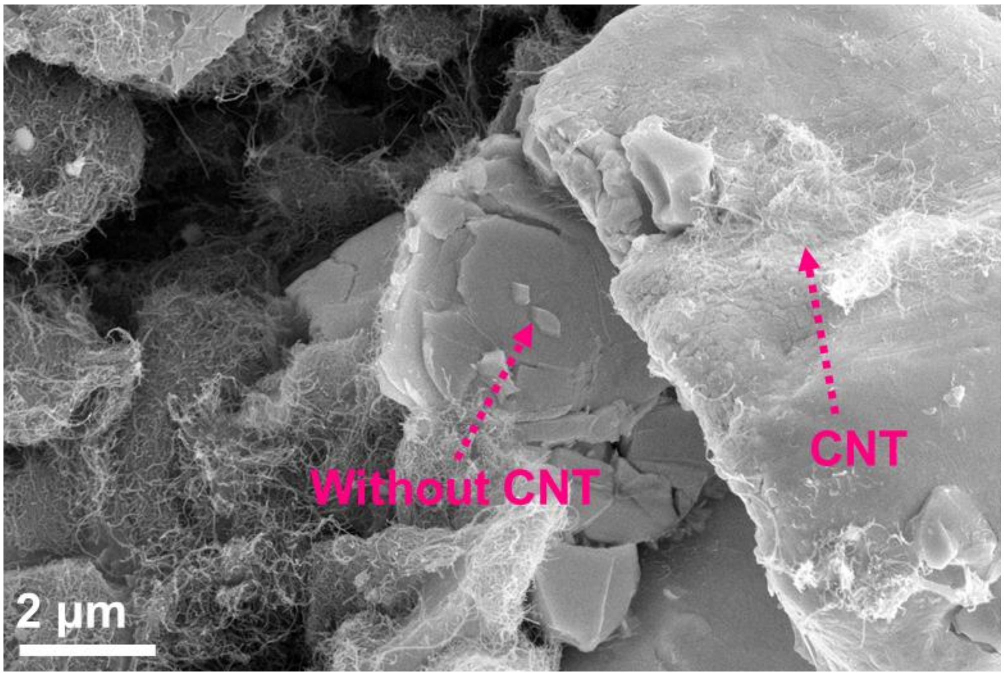

Fig. S9. The SEM image of Bi@CNT-2.61 maintained for 5 min at 20 Mpa.

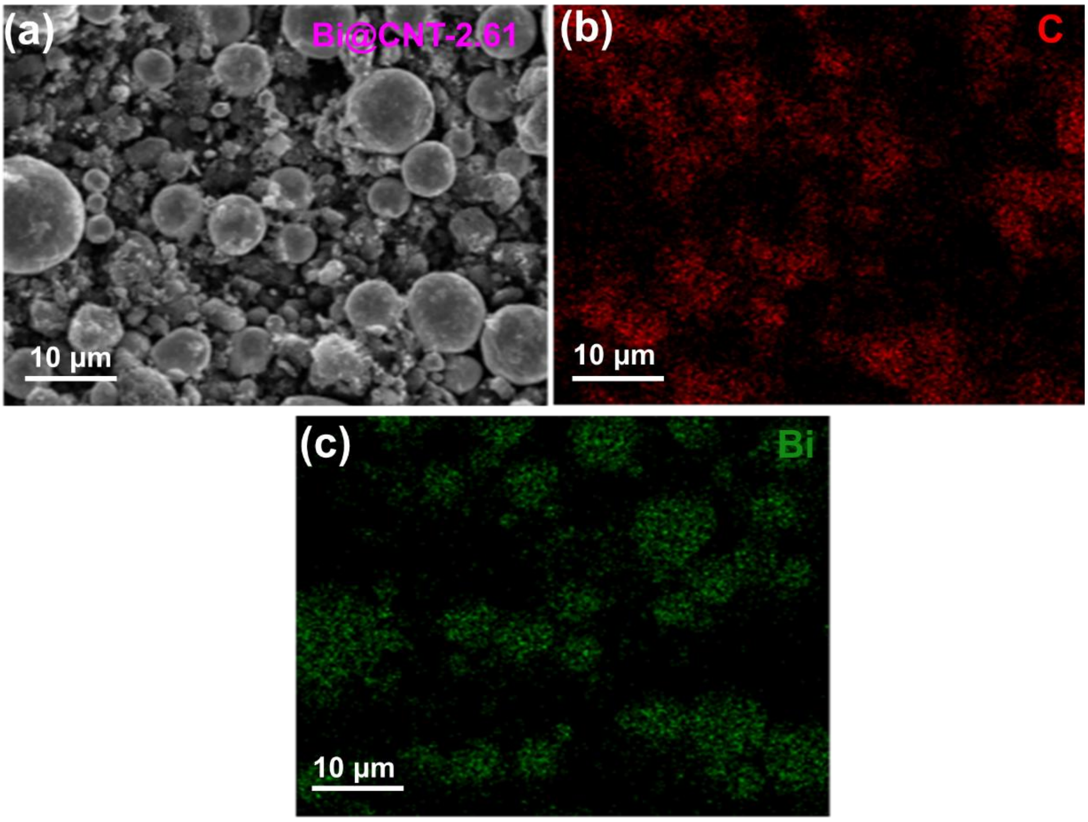

Fig. S10. SEM-EDS images of Bi@CNT-2.61 materials.

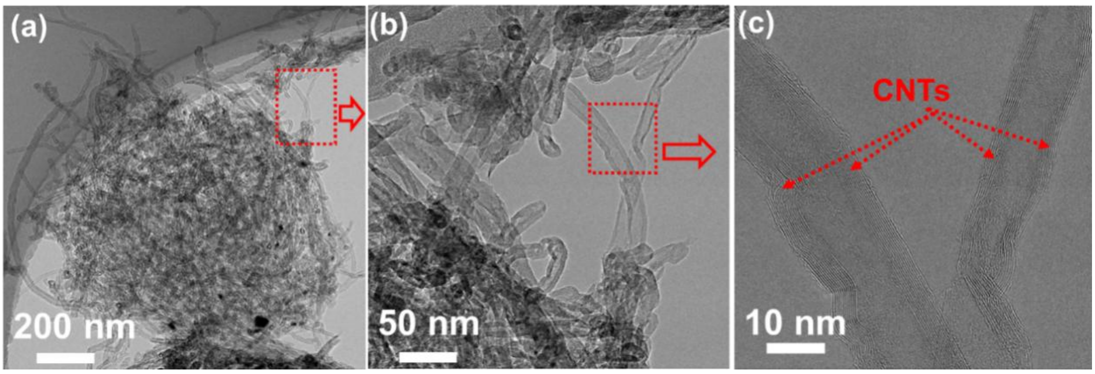

Fig. S11. TEM images of the pure CNTs.

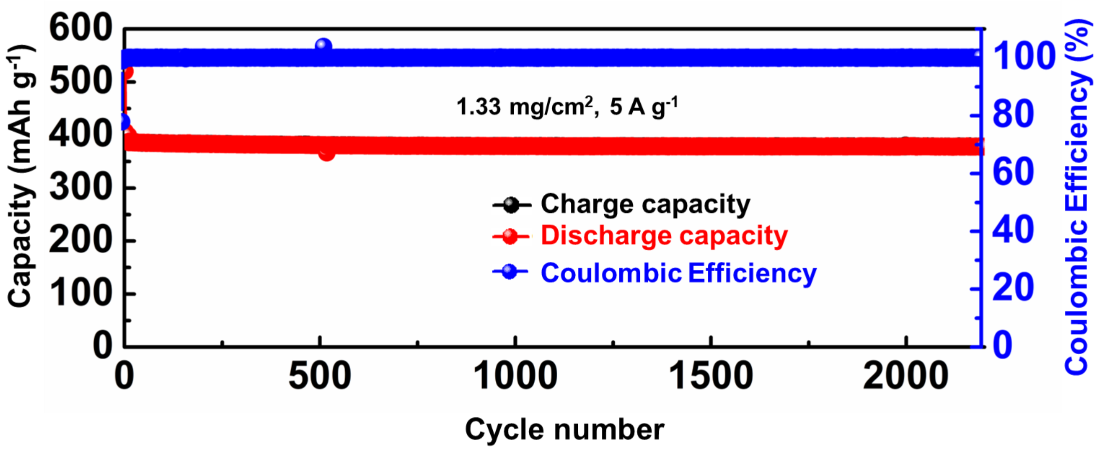

Fig. S12. Long-term cycle curve of Bi@CNT-2.61 electrode at 5 A g^{-1} with a mass loading of 1.33 mg/cm^2.

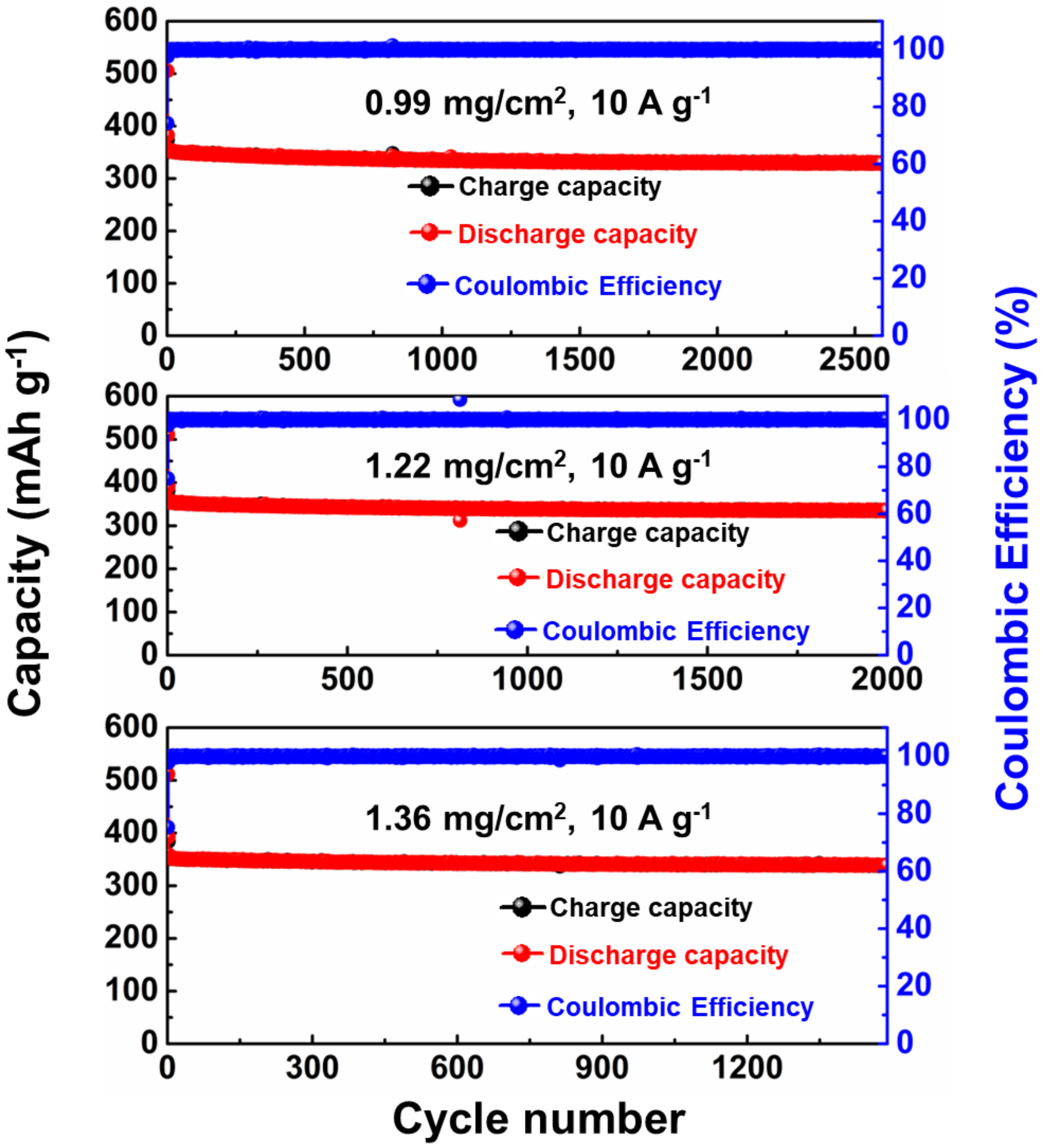

Fig. S13. Long-term cycle curves of Bi@CNT-2.61 electrode at 10 A g^{-1} with different mass loads.

Table S5. Comparisons of Half-cell performance of Bi-based anodes reported in literatures for SIBs.

Samples	Voltage window	Capacity (mAh g^{-1}).	Long-term cycling stability (mAh g^{-1}@cycles)	Electrolyte	references
Bi@NPC-850-U	0.01-1.5 V	290.3, 271.5, 267, 263.4, 259.8, 254.2, 247.5, and 231.3 at 0.2, 0.6, 1, 2, 5, 10, 20, and 35 A g^{-1}, respectively.	243.8@2000 at 10 A g^{-1}.	1 M $NaPF_6$ in diglyme(DIG).	4
FBi@NC	0.01-1.8 V	385.8, 386.3, 386.4, 385.7, 385.2, 384.4, 383.8, 382.4, 380.5, 377.1, and 368.2 at 0.1, 0.5, 1, 3, 5, 8, 10, 15, 20, 25, and 30 A g^{-1}, respectively.	318.8@10,000 at 5 A g^{-1}, 328.8 @8000 at 10 A g^{-1}, 246.8@5000 at 20 A g^{-1}.	1 M $NaPF_6$ in 1, 2-dimethoxyethane (DME).	17
Bi@N-C	0.01-1.5 V	300, 282, 262, 252, 240, 211, 178 at 1, 2, 5, 10, 20, 50 and 100 A g^{-1}, respectively.	235@2000 at 10 A g^{-1}, 300@400 at 1 A g^{-1}.	1 M $NaPF_6$in 1, 2-dimethoxyethane (DME).	29
Bi@NS-C	0.01-1.5 V	372.9, 376.9, 383.4, 389.8, 388.3, 360 at 1, 2, 5, 10, 20 and 30 A g^{-1}, respectively.	388.9@1300 at 10 A g^{-1}, 366.3@2600 at 1 A g^{-1}.	1 M $NaPF_6$ dissolved in diglyme (DIG).	30
Bi@3D-CFs	0.01-1.3 V	408, 382, 377, 368, 365, 361, 359, 355, 348, 331, and 311 at 0.5, 1, 2, 5, 10, 20, 30, 45, 60, 80, and 100 A g^{-1}, respectively.	349@12,000 at 5 A g^{-1}.	1 M $NaPF_6$ in 1, 2-dimethoxyethane (DME).	31

Bi NTs	0.01-1.5 V	382, 378, 377, 369, and 350 at 1, 10, 20, 50, and 100 A g^{-1}, respectively.	200@65,000 at 50 A g^{-1}, 355@15,000 at 20 Ag^{-1}, 351.7@5000 at 1 A g^{-1}.	1M $NaPF_6$ in 1, 2-dimethoxyethane(DME)	32
3DBS aerogel	0.01-1.6 V	375.6, 332.0, 341.1, 344.0, 344.5, 342.3 and 330.6 at 0.5, 1, 2, 5, 10, 20 and 30 C (1C=386 mA g^{-1}), respectively.	339.1@2000 at 10 C (10 C= 3.86 A g^{-1}).	1.0 M NaPF6 in diglyme (DIG).	33
Bi@CNT-2.61	**0.01-1.2 V**	**400.1, 394.0, 401.2, 403.6, 402.1, 395.7, 390.4, 382, 366.5, 340.8 and 293.6 mAh g^{-1} at 0.1, 0.2, 0.5, 1, 2, 5, 10, 20, 30, 40 and 50 A g^{-1}, respectively.**	**377.6@2200 at 5 A g^{-1}, 329.3, 335.5 and 338.9@2600, 2000 and 1490 at 10 A g^{-1} with the mass loadings of 0.99, 1.22 and 1.36 mg/cm^2, respectively. 248.1 and 277.3@5450 and 3250 at 50 A/g with the mass loadings of 0.89 and 1.36 mg/cm^2, respectively.**	**1 M $NaPF_6$ in 1, 2-dimethoxyethane (DME).**	**This work**

Refer to **Table S5** (continued)

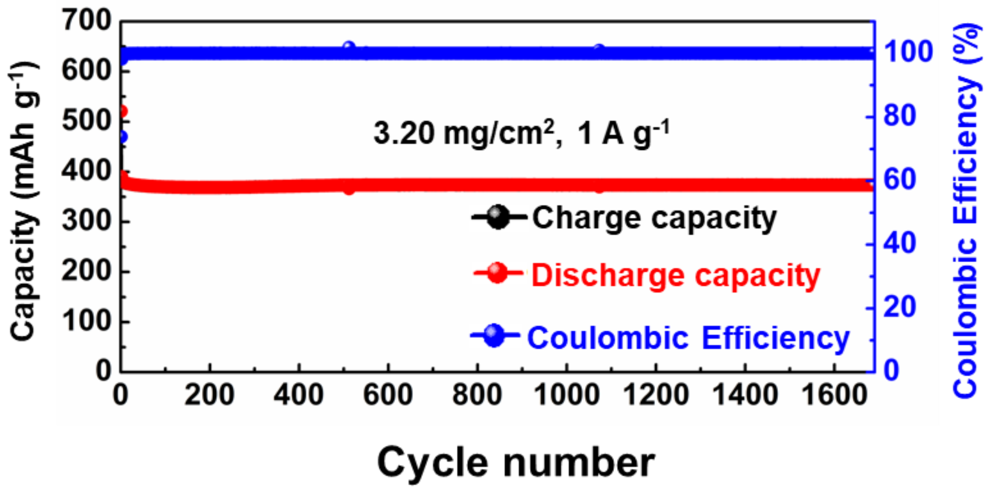

Fig. S14. Cycling performance of Bi@CNT-2.61 electrode with a high mass loading at 1 A g^{-1}.

$$i=a\vartheta^{b}$$
Equation S2

$$\log i=b\log\vartheta+\log a$$
Equation S3

In general, the Na^+ storage mechanism can be described by the relationship between the scanning rate (v) and the peak current (i) according to Equation S2: $i = a\nu^{b}$, where a and b are the empirical parameters.

The value of b which can be computed from log(i)–log(v) curves (Equation S3) is used to determine the electrochemical behavior: b=1 represents a completely capacitive process, while b= 0.5 indicates a completely diffusion-controlled process.

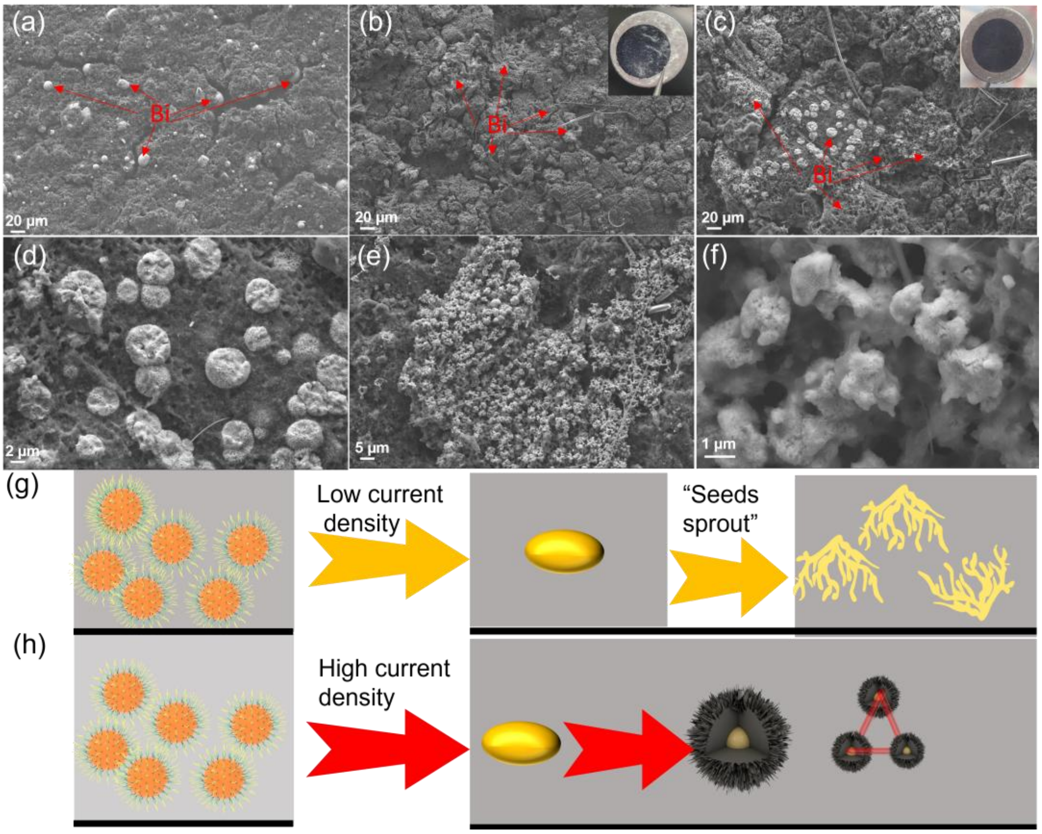

Fig. S15. (a) SEM image of fresh electrode. (b) SEM image of Bi@CNT-2.61electrode after 100 cycles at 0.2 A g^{-1}. (c) SEM image of Bi@CNT-2.61electrode after 5450 cycles at 50 A g^{-1}. (d-f) are the partial enlargements of (c). (g) is the seed-sprout-like image which is utilized to describe the morphologies of Bi in Bi@CNT-2.61 of (a, b). (h) is the-sea-urchin like image which is utilized to describe the morphologies of Bi in Bi@CNT-2.61of (c)~(f).

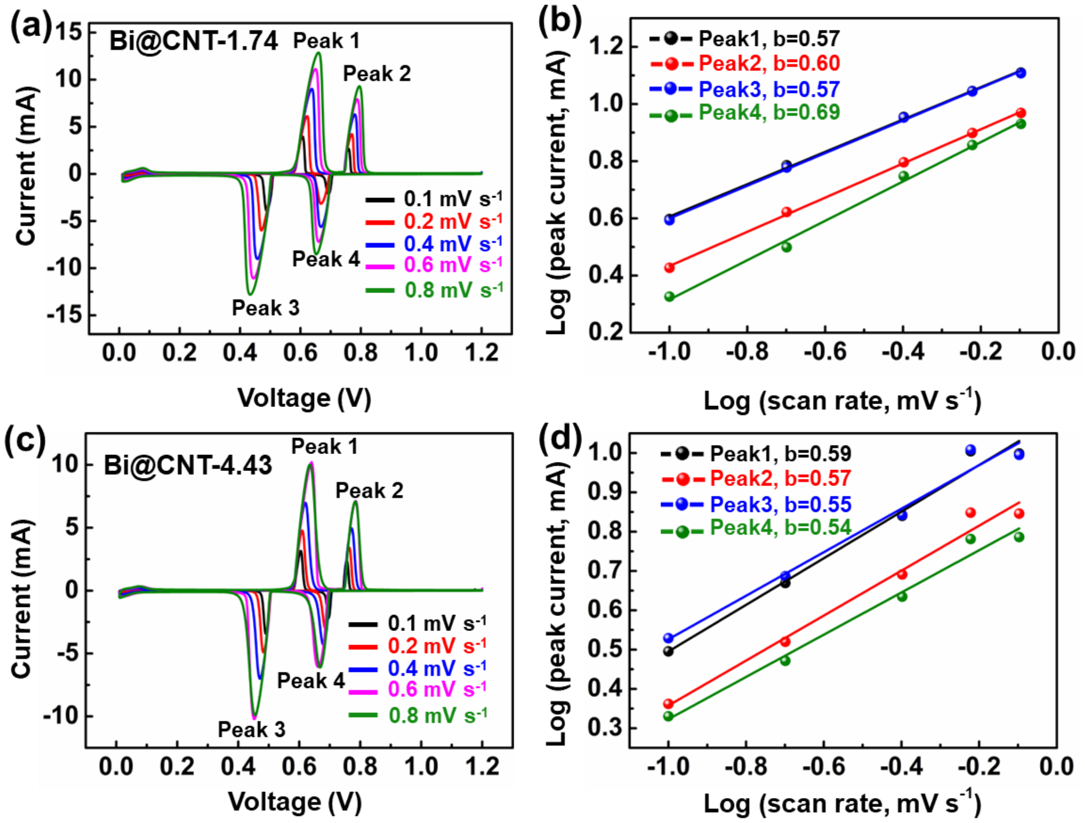

Fig. S16. (a, c) CV curves of Bi@CNT-1.74 electrode and Bi@CNT-4.43 electrode at various scan rates, respectively. (b, d) Plots of the corresponding log(i) versus log(v) of peak1, peak2, peak3, and peak4 from Bi@CNT-1.74 electrode and Bi@CNT-4.43 electrode, respectively

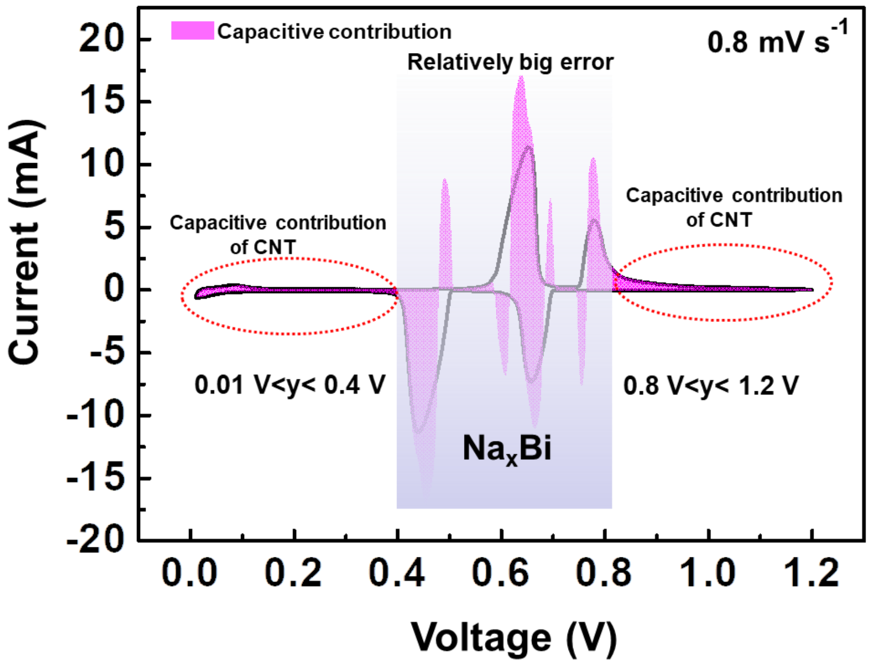

Fig. S17. Pseudocapacitive contribution of Bi@CNT-2.61 electrode at a scanning rate of 0.8 mV s^{-1}.

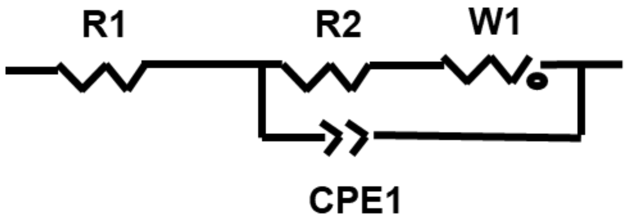

Fig. S18. The equivalent Randles circuit. Thereinto, R1 is the total resistance of the electrolyte, separator, electrical contacts, and the SEI film; R2 is the charge-transfer resistance; W1 is the Warburg impedance connected with the Na^+ diffusion process; CPE1 represents the double-layer resistance.

Table S6. Simulated impedance of the Bi, CNTs and Bi@CNT materials.

Samples	R1	R2
Bi	4.68	12.25
CNTs	3.24	0.74
Bi@CNT-1.74	3.76	16.41
Bi@CNT-2.61	2.74	0.72
Bi@CNT-4.43	3.69	66.34

$$D_{Na^+}=\frac{R^2T^2}{2C^2A^2\sigma^2F^4n^4}$$

Equation S4

In Eq (S4), R, T, n, F, A, C and σ correspond to the gas constant (8.314 JK^{-1} mol^{-1}), absolute temperature (303.15 K), the number of transferred electrons per mole, the Faraday constant (96 500 C mol^{-1}), the effective electrode area (cm^2), the sodium ion concentration in the electrode (mol cm^{-3}) and the Warburg factor (Ω $s^{-1/2}$), respectively.

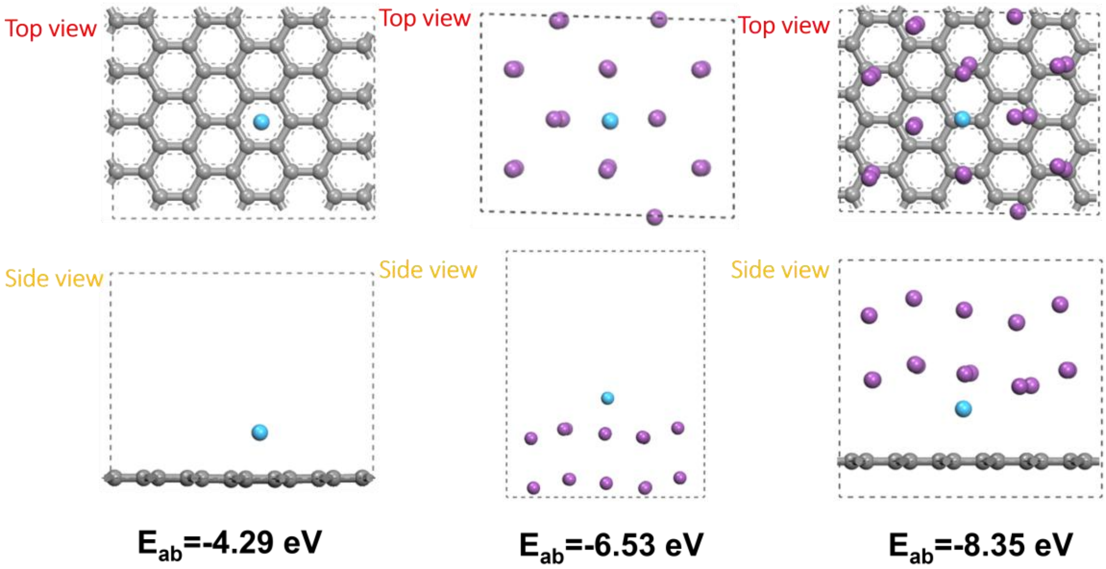

Fig. 19. Adsorption models for Na^+ adsorption energies on the surfaces of C, Bi, and Bi@CNT materials.

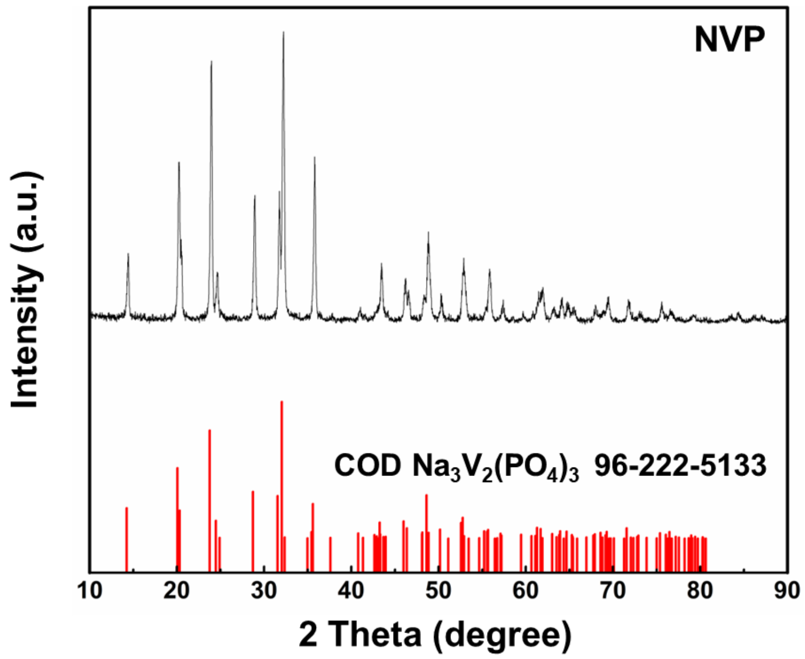

Fig. S20. The XRD pattern of the NVP.

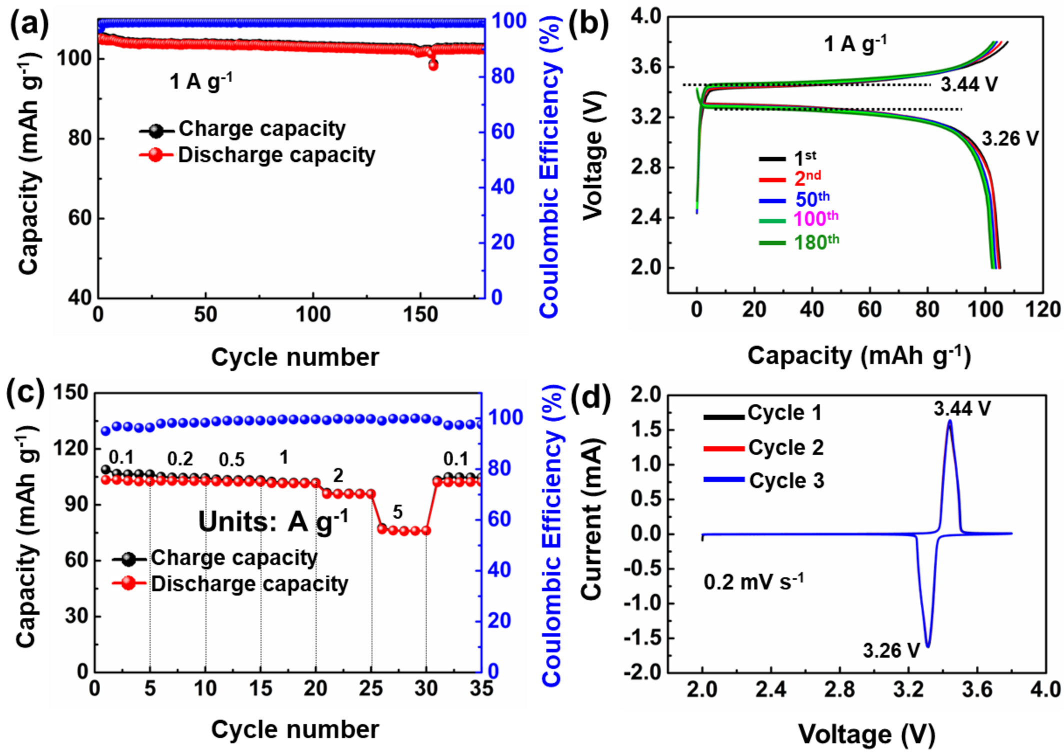

Fig. S21. Electrochemical results of NVP in a half-cell. (a) Cycling performance at 1 A g^{-1}. (b) Charge/discharge profiles at 1 A g^{-1}. (c) Rate performance at various current densities. (d) The initial three CV curves at the scan rate of 0.2 mV s^{-1}.

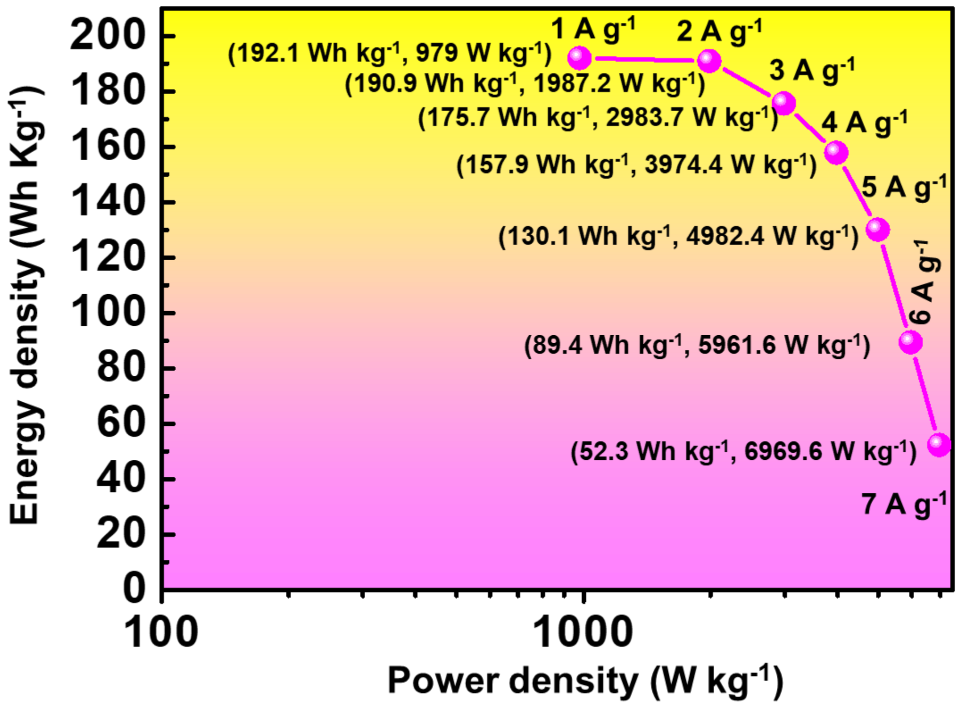

Fig. S22. Ragone plot (Energy density vs. Power density) of the NVP//Bi@C-2.61 full cell in this work.

Table S7. Comparisons of full battery performance with Bi-based anodes for Na-ion batteries reported in literature for SIBs.

Full cell cathode//anode	Cycling performance[a]	Rate capacity[b]	Energy density[c] (Wh kg^{-1})	Mass ratio (cathode: anode)	references
ops-Bi/C// $Na_3V_2(PO_4)_3$ (NVP)	102.00/ 100/ 0.1	102 and 90/ 0.1 and 1, respectively.	$174_{(total)}$/0.1	3: 1	13
Bi@NC//$Na_3V_2(PO_4)_3$NVP	223.3/ 200/ 1	246.7, 231.0, 223.4, 210.4, 198.2, and 180.2/ 0.2, 0.5, 0.8, 1.0, 2.0 and 5.0, respectively.	$125_{(total)}$/1	3.5: 1	14
Bi@N-C//NVP/C	240/ 800/ 1	320, 270, 263, 254, 243, 231, and 223/ 0.05,0.1, 0.4, 0.8, 1.2, 1.6, and 2.0, respectively.	$154_{(total)}$/0.05	1.4: 1	15
Bi@NC// $Na_3V_2(PO_4)_3$@C	57/ 2000/ 1	91,81, 73, 69, 67, and 65/ 0.1, 0.2, 0.4, 0.6, 0.8, and 1.0, respectively.	-	3.5: 1	16
Sn-Bi@C// NVP	56/ 300/ 1	73.4, 67.3, 64.9,62.9, and 58.5/ 0.1, 0.2, 0.5, 1.0, and 2.0, respectively.	$251.2_{(total)}$/1	4: 1	19
Bi@CNT-2.61//NVP	**189.66/ 445/ 1 133.89/ 400/ 5**	**195.4, 184.8, 176, 157.2, 132.4, 87.7, and 53.5/ 1, 2, 3, 4,5, 6, and 7, respectively.**	**$192.1_{(total)}$/1**	**1.9: 1**	**This work**

a) The cycling performance is summarized as capacity (mAh g^{-1})/cycle number/current density (A g^{-1}) used in literature and this work for SIBs.

b) The rate capability is summarized as capacity (mAh g^{-1})/current density (A g^{-1}) used in literature and work for SIBs.

c) The energy density is summarized as energy density (Wh kg^{-1})/current density (A g^{-1}) used in literature and this work for SIBs